

Original Research Article**Synthesis, characterization and electrochemical studies on $\text{Li}_4\text{Fe}(\text{CN})_6$ as cathode material for Li-ion batteries****ABSTRACT**

An easy and cost effective method of synthesis of $\text{Li}_4\text{Fe}(\text{CN})_6$ has been reported. The material, as obtained, has been characterized by UV-VIS, FTIR, powdered XRD and SEM. Cyclic-voltametry and charge-discharge studies were carried out for electrochemical characterization of the synthesized material. A laboratory model Li-ion cell was fabricated using $\text{Li}_4\text{Fe}(\text{CN})_6$ as cathode, lithium metal as anode and 1 molar LiClO_4 solution in ethylene carbonate and dimethyl carbonate (1:1) mixture as electrolyte. The cell shows an open circuit potential of 3.03 volts vs. Li and a discharge capacity of 90 mAhg^{-1} (theoretical capacity, 112 mAhg^{-1}) in the first few cycles at 0.15 C rates. The charge-discharge behaviour remains practically unaltered up to 20 cycles. Thus $\text{Li}_4\text{Fe}(\text{CN})_6$ may be considered as a promising cathode material for Li-ion battery.

Keywords: $\text{Li}_4\text{Fe}(\text{CN})_6$ cathode; cost effective method; low temperature calcinations; charge-discharge; Li-ion battery.

1. INTRODUCTION

Lithium-ion batteries are one of the most powerful [1], and popular storage systems due to highest energy-to-weight ratios, no memory effect, and slight energy loss when not in use [2]. Beyond consumer electronics, lithium-ion batteries are being used for military, electric vehicles and aerospace

applications because it has the greatest electrochemical potential and provides the largest energy density, 125-150 Whkg⁻¹ [1].

Commercial lithium-ion batteries contain LiCoO₂ as the cathode material, in which the component element cobalt is very expensive and toxic [3, 4]. As a result large scale applications using this material is limited. Therefore, scientists are looking for new cathode materials, which are less expensive and compatible with the environment [4]. During last decade, a number of new cathode materials were proposed. However, none of them are found suitable for commercial applications due to different critical issues, such as toxicity, higher resistivity, smaller specific capacity, low operating potential, lower cyclability and large capacity fading upon cycling. Among them layered LiMnO₂ and spinel LiMn₂O₄ compounds have been drawn more attention as alternative cathode materials for lithium-ion batteries [5-10]. But it has low diffusion coefficient of lithium-ion and large capacity fading upon cycling.

Recently, lithium iron phosphate (LiFePO₄) become an attractive alternating cathode material for rechargeable lithium-ion batteries [11-16], due to low cost starting materials, environment friendly, excellent cycling performances, high theoretical capacity (170 mAhg⁻¹), high safety, good operating voltage and high temperature performance [2, 11-14]. Again the main disadvantage associated with this material is its low electronic conductivity and low diffusion coefficient of lithium ions, which lead to its poor rate capability [13, 14]. Some efforts to increase its conductivity have been made after doping with higher valence metal cations, like Ti⁴⁺, Ga³⁺, Zr⁴⁺, W⁶⁺, V³⁺ etc. and a few fold enhancements in conductivity is reported in the cost of intrinsic capacity [17-20]. It will be interesting to increase the conductivity without losing its capacity and that can be done by synthesizing nano LiFePO₄ through different particle size controlled techniques like water-based [21-26], sol-gel [27-30], sonochemical [31], solvothermal [32], **Error! Reference source not found.** ionothermal [33], and in-situ carbon coating via solid-state synthetic method [34]. Most of the reported methods are lengthy and expensive. There are few reports available on the synthesis of nano LiFePO₄ [16, 24, 25, 31], over large surface area carbon powder with better performance and cyclability.

However, it is very much difficult to synthesize pure LiFePO₄ in solid state or sol-gel methods because in these methods an inert atmosphere is required during calcinations to protect oxidation of Fe²⁺ to Fe³⁺ [11-20]. Therefore nitrogen or argon gas and an instrumental set up are required to make inert atmosphere which is costly and difficult also.

Here, we report a new cathode material Li₄Fe(CN)₆ [35], which is synthesized in a simple route without using inert atmosphere and high temperature calcinations [15-25]. Material retains its discharge capacity close to its theoretical value 112 mAhg⁻¹, which is slightly lower than the commercial material [36]. On the other hand, Li₄Fe(CN)₆ is soluble in water, and thus it can be used as liquid cathode [37], in aqueous lithium-ion battery.

2. MATERIALS AND METHOD

2.1 Material Synthesis Procedure

Concentrated solutions of K₄Fe(CN)₆·3H₂O (BDH, USA, 99%) (6 g in 25 ml) and LiClO₄ (Alfa-Aesar, USA, 99%) (6.045 g in 15 ml) were prepared separately. They were then mixed together at room temperature under constant stirring condition. A white crystalline precipitate of KClO₄ was appeared (because the solubility of KClO₄ in water is 1.5 g/100 ml at 25 °C [38]). The precipitate was filtered and the filtrate was cooled down to 10 °C and kept overnight. Again a white precipitate of KClO₄ was appeared which was collected by filtration and the remaining solution was concentrated by evaporating the water at a temperature of 60-70 °C with the help of vacuum evaporator. Then concentrated solution was cooled down to 10 °C and left for 12 hours. Again a crystalline precipitate of KClO₄ was appeared. The precipitate was filtered out and the process was repeated to remove KClO₄ completely. The filtrate containing Li₄Fe(CN)₆ was then evaporated to dryness and sintered at a temperature of 180 °C. Now the synthesized anhydrous material was cooled down to room temperature and kept in a sealed moisture free bottle for further analysis.

2.2 Thermal Gravimetric Analysis (TGA)

Thermo-gravimetric analysis of the solid material, obtained after dehydration of filtrate containing $\text{Li}_4\text{Fe}(\text{CN})_6$, was made using a Perkin-Elmer TGA/DTA thermal analyzer in nitrogen atmosphere at a heating rate of 20°Cmin^{-1} and the graph is shown in Fig. 1.

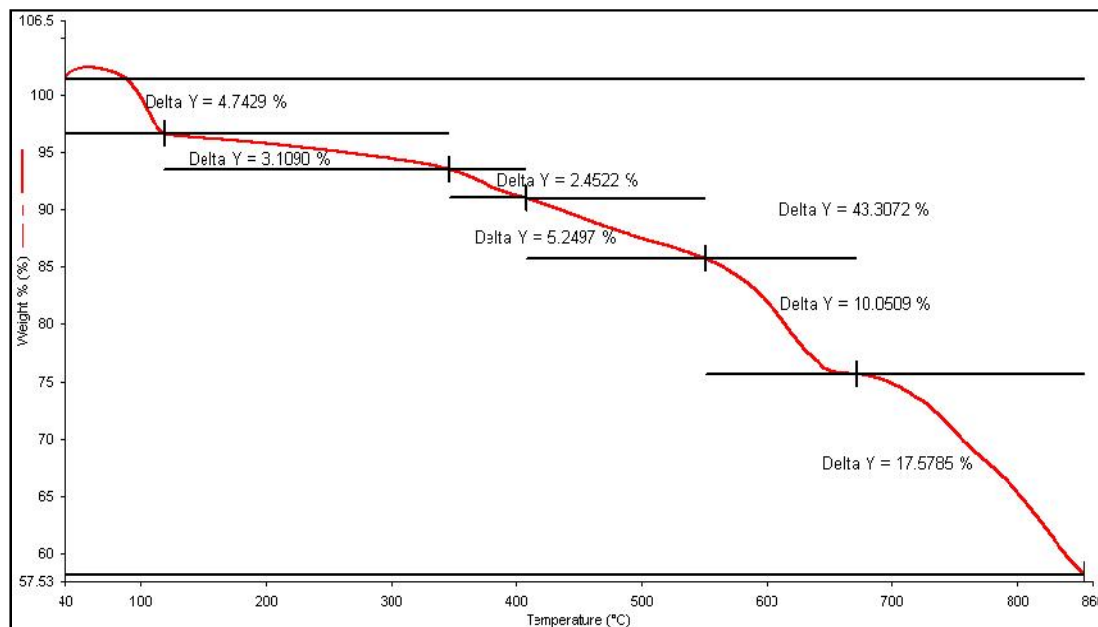


Fig. 1. TGA of solid material obtained after dehydration of filtrate containing $\text{Li}_4\text{Fe}(\text{CN})_6$.

From the figure, it is seen that 4.7% mass loss occurred due to water loss within 120°C . Above this temperature mass loss occurred stepwise due to dehydration and decomposition of $\text{Li}_4\text{Fe}(\text{CN})_6$. Therefore, sintering the material within 180°C can produce dehydrated material because within this temperature the material does not decompose, but undergoes dehydration only.

2.3 Characterization Part

$\text{Li}_4\text{Fe}(\text{CN})_6$ was characterized by UV-Visible spectrophotometer (OPTIZEN POP), Fourier Transform Infrared (FTIR, FTIR-8400S, Shimadzu, Japan), Powdered X-ray diffraction (XRD, Ultima III Rigaku $\text{Cu K}\alpha$, $\lambda=1.5406\text{ \AA}$) and Scanning Electron Microscope (SEM, JEOL, JSM-6360, UK).

Cyclic-voltammetry and Charge-discharge studies were carried out by a Galvanostat/Potentiostat (VersaStatTM II, Princeton Applied Research). The reversibility and the storage capacity of the synthesized material were studied by cyclic-voltammetry and chrono-amperometry studies, respectively after preparing a laboratory model cell. The cathode mixture was prepared by mixing the synthesized material (80 wt %) with carbon conductive additive i.e., carbon black (Alfa Aesar, USA, 99.9%) (8 wt %), graphite powder (Alfa Aesar, USA, 99.99%) (8 wt %) and Polyvinylidene fluoride (Aldrich, USA) (4 wt %) in N-methyl pyrrolidone (Merck, USA, 99.5%) as solvent to make homogeneous slurry [26-34]. This slurry was then spread over a thin aluminum foil so that they are equally distributed. N-methyl pyrrolidone and moisture was removed by heating the foil at 80°C with the help of a vacuum evaporator. The positive electrode was ready for cell fabrication upon cooling down to room temperature. Li (Aldrich, USA, 99.9%) ribbon pasted on a nickel plate was used as anode. One molar LiClO_4 (Alfa Aesar, 99%) solution in equal solvent mixture of Ethylene carbonate (Sigma-Aldrich, USA, 98%) and Dimethyl carbonate (Sigma-Aldrich, USA, 99%) and porous polypropylene (PP) film soaked with this electrolyte, was used as electrolyte and separator, respectively. The cell was assembled inside a glove bag after removing air and moisture by purging argon gas.

3. RESULTS AND DISCUSSION

3.1 UV-Visible spectroscopy

The UV-Visible spectrum of aqueous solution containing $\text{Li}_4\text{Fe}(\text{CN})_6$ is shown in Fig. 2.

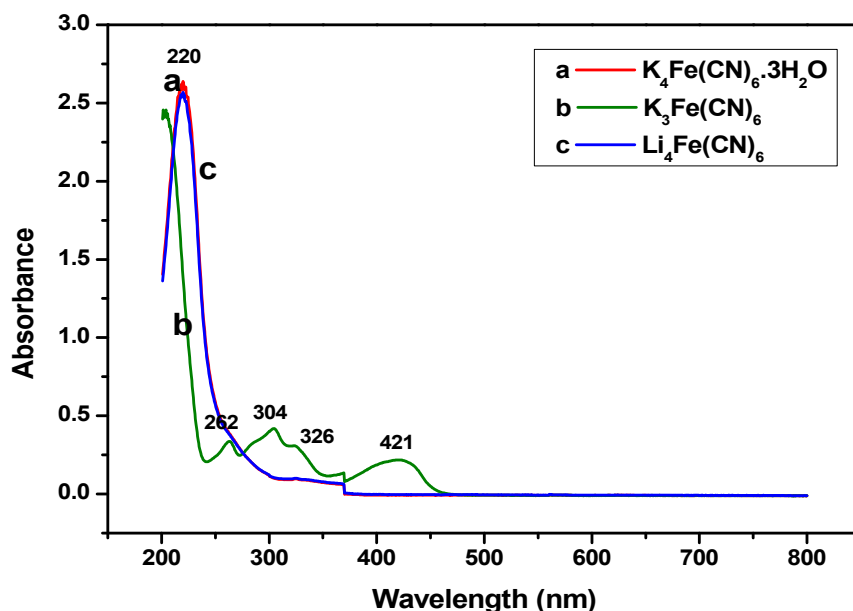


Fig. 2. UV-Visible spectroscopy of $\text{K}_4\text{Fe}(\text{CN})_6 \cdot 3\text{H}_2\text{O}$, $\text{K}_3\text{Fe}(\text{CN})_6$ and $\text{Li}_4\text{Fe}(\text{CN})_6$.

From Fig. 2, it is found that an intense absorption peak at 220 nm, attributed to the presence of ferrocyanide group which overlaps with absorption maxima of the commercial $\text{K}_4\text{Fe}(\text{CN})_6 \cdot 3\text{H}_2\text{O}$ crystals. On the other hand, the synthesized materials is free from ferricyanide impurity, as it is confirmed from the UV-Vis data (Fig. 2) of commercial $\text{K}_3\text{Fe}(\text{CN})_6$ (BDH, USA, 99%) [39, 40].

3.2 Fourier Transform Infrared (FTIR) spectroscopy

The FTIR spectrum of $\text{Li}_4\text{Fe}(\text{CN})_6$ crystal shown in Fig. 3 shows its characteristic peaks at $2044\text{--}2071\text{ cm}^{-1}$, 552 cm^{-1} and 419 cm^{-1} due to the $\nu(\text{CN})$ of $\text{Fe}(\text{CN})_6^{4-}$, $\delta(\text{FeCN})$ and $\nu(\text{FeC})$, respectively, which matches well with the literature data [41-44].

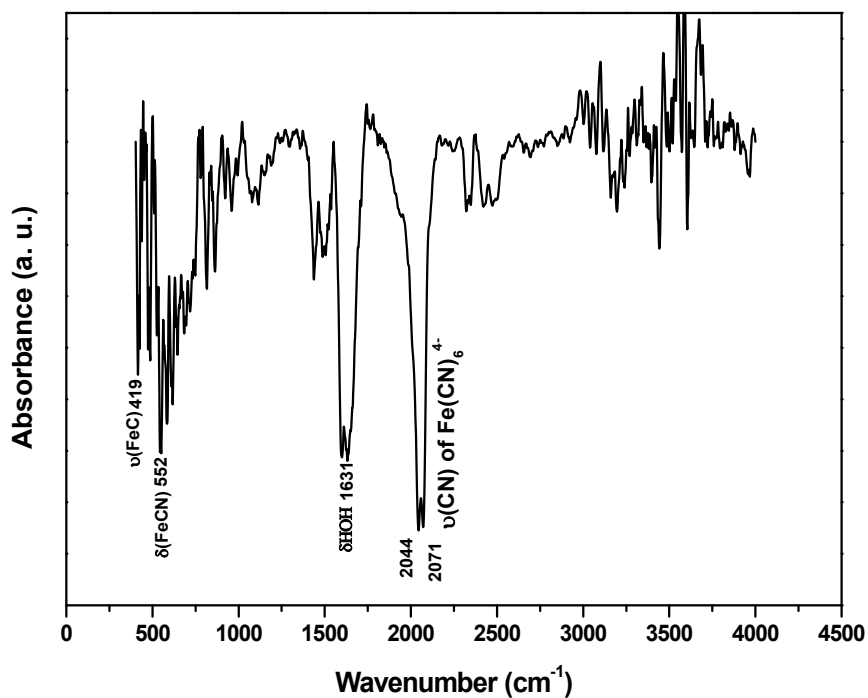


Fig. 3. Fourier Transform Infrared (FTIR) spectroscopy of $\text{Li}_4\text{Fe}(\text{CN})_6$.

3.3 Powdered X-ray diffraction

The powdered XRD of the synthesized material was recorded in the range of $2\theta = 10^\circ$ - 50° with scan rate of 5°min^{-1} . The XRD pattern of the synthesized $\text{Li}_4\text{Fe}(\text{CN})_6$ is shown on Fig. 4.

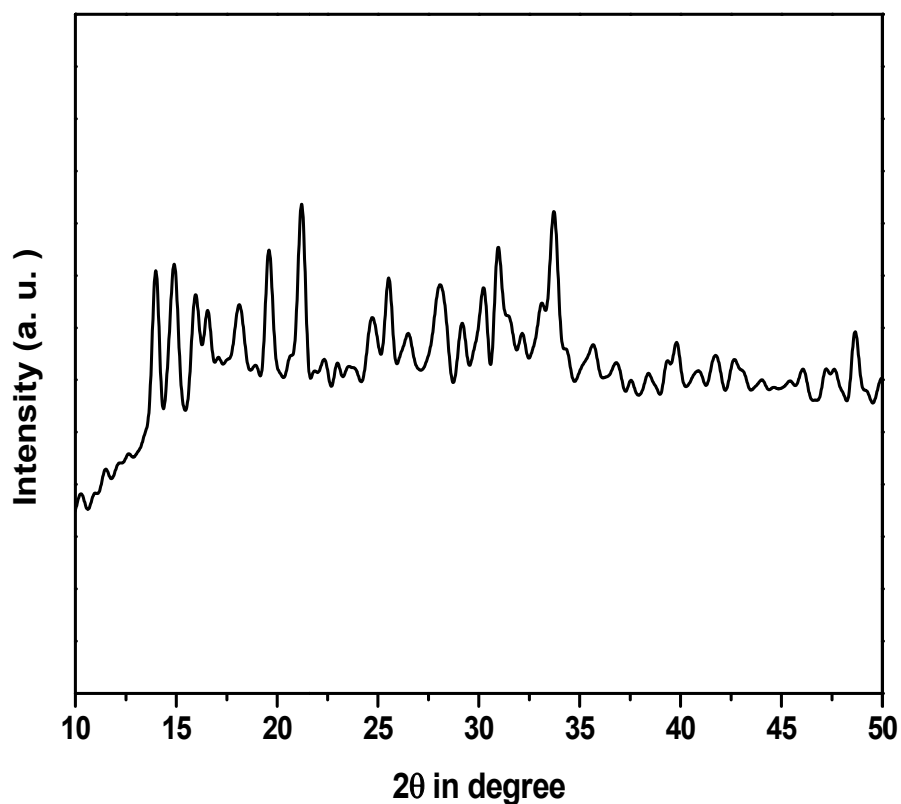


Fig. 4. Powdered X-ray diffraction of $\text{Li}_4\text{Fe}(\text{CN})_6$.

There is no regular sharp peak in the XRD pattern indicating the formation of both crystalline and amorphous phase. Since there is no literature report available on the XRD pattern of $\text{Li}_4\text{Fe}(\text{CN})_6$, we are not able to compare with the literature data. Crystal structure shall be determined from the single crystal data, which is under investigation and may be reported later.

3.4 Scanning Electron Microscopy (SEM)

The surface morphology and particle size of the synthesized material were studied from the SEM images, shown in Fig. 5.

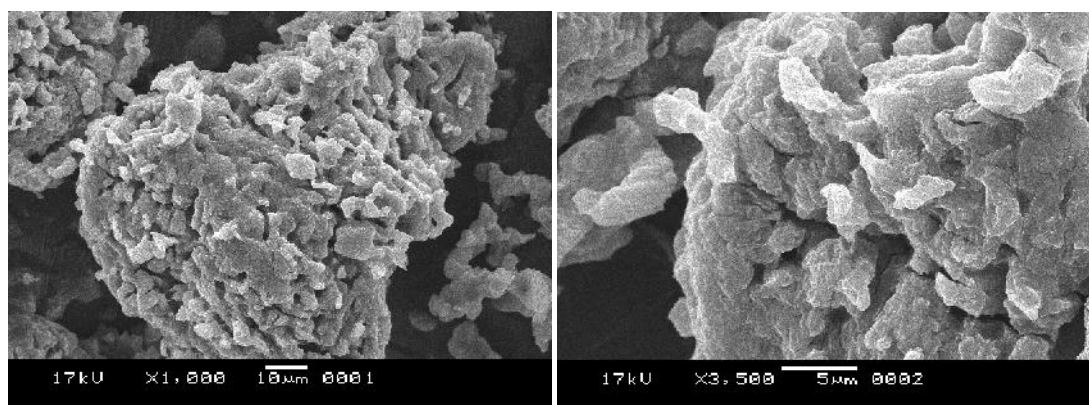


Fig. 5. SEM images of $\text{Li}_4\text{Fe}(\text{CN})_6$.

From the images it is revealed that the particles are agglomerated in nature with average particle size in the range of 3-5 μm .

3.5 Electrochemical study

The cyclic voltammogram of the synthesized $\text{Li}_4\text{Fe}(\text{CN})_6$ cathode were recorded, as shown in Fig. 6, in the potential window of 1.5 V to 4.8 V vs. Li at a scan rate of 0.5 mVs^{-1} .

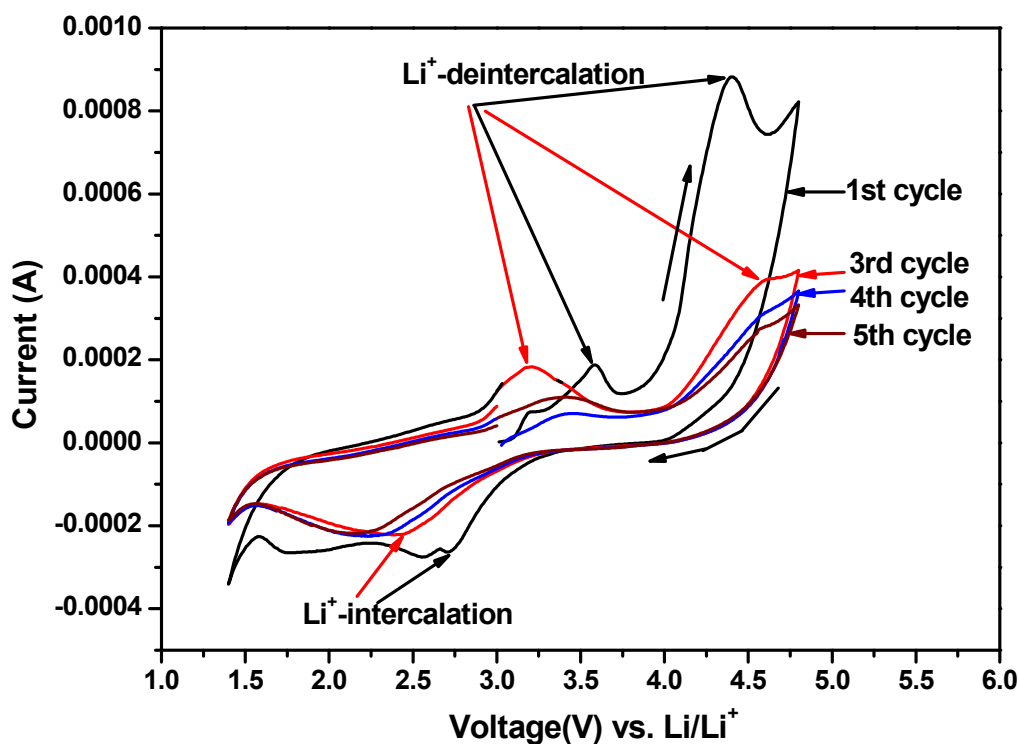


Fig. 6. Cyclic voltammetry of $\text{Li}_4\text{Fe}(\text{CN})_6$ in 1 Molar LiClO_4 solution in EC+DMC(1:1) mixture vs. Li/Li^+ at the scan rate of 0.5 mVs^{-1} .

In the first cycle during forward scan two oxidation peaks appeared at 3.58 volt and 4.4 volt and the corresponding two reduction peaks are observed around 2.71 volt. But in the next cycle, slight changes in the peak positions were observed. It should be noted that the multi peaks converges in to a single peaks in subsequent cycles. The extra peak might be due to structural changes within the molecule, because only a single oxidation and reduction peak is expected for $\text{Li}_4\text{Fe}(\text{CN})_6$. More importantly, cyclic voltammetry study reveals that the system is reversible in nature and reversibility retained in the subsequent cycles.

Galvanostatic charge-discharge behaviour of the assembled cell using $\text{Li}_4\text{Fe}(\text{CN})_6$ as cathode shown in Fig. 7, were recorded at a rate of 0.15 C and 0.30 C.

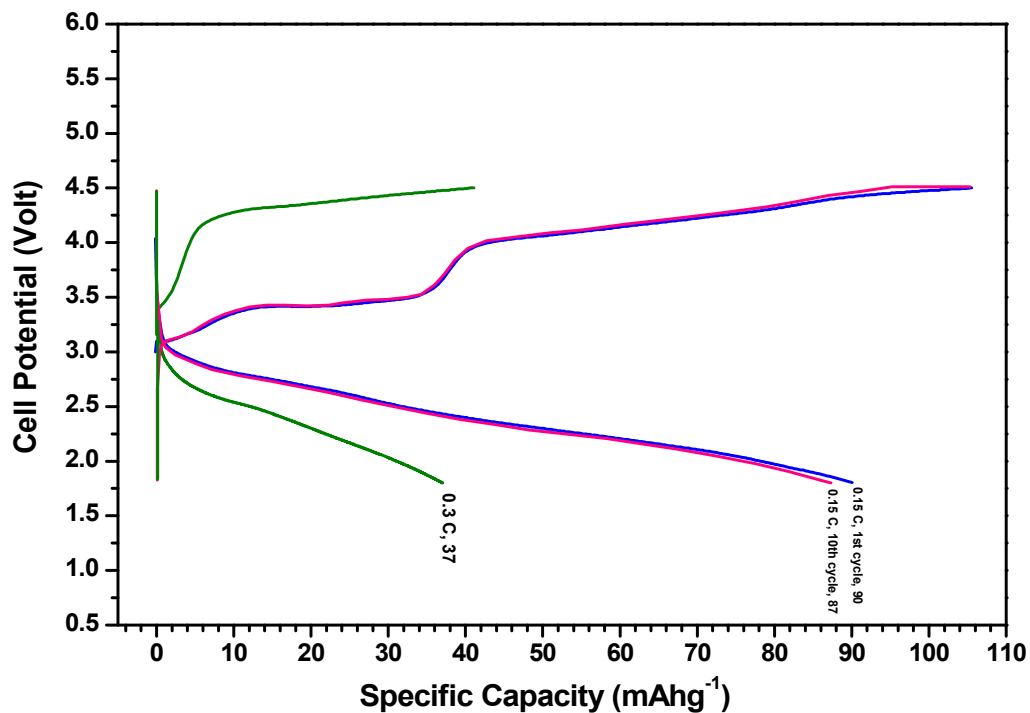


Fig. 7. Charge-discharge behaviour of $\text{Li}_4\text{Fe}(\text{CN})_6$ vs. Li/Li^+ at 0.15 C and 0.30 C current densities.

At low rate (0.15 C), the cell shows the maximum faradic capacity of 90 mAhg^{-1} , which is about 80% of the theoretical value i.e., 112 mAhg^{-1} and the value practically remain unaltered up to 15-20 cycles as shown in Fig. 8. At high drain condition the cell delivered a capacity of 37 mAhg^{-1} , due to migratory limitation of the Li^+ ions.

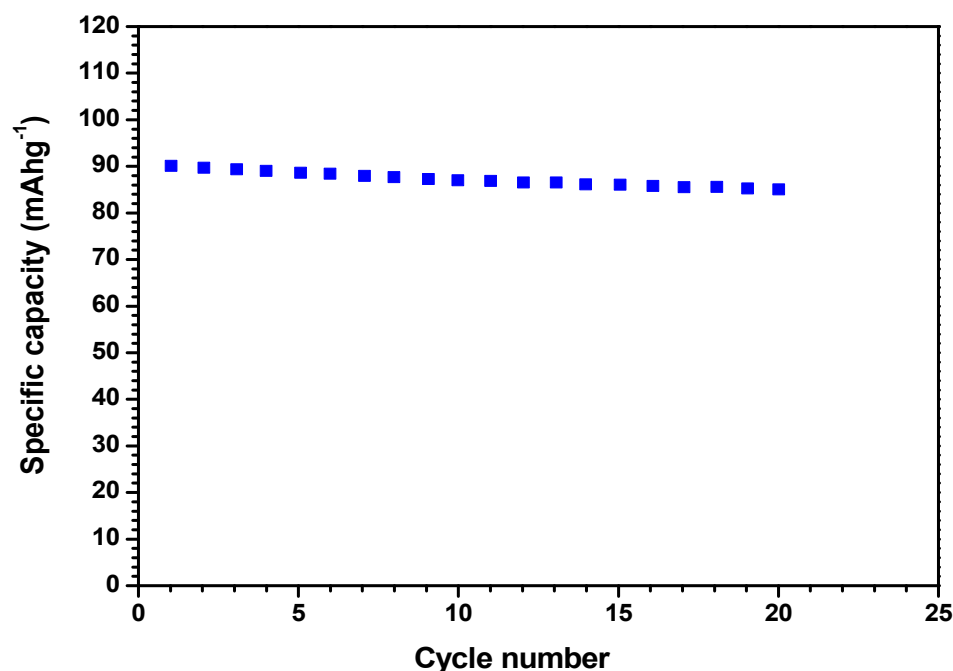


Fig. 8. Discharge capacities of $\text{Li}_4\text{Fe}(\text{CN})_6$ cathode vs. cycle number at 0.15 C current density.

4. CONCLUSION

$\text{Li}_4\text{Fe}(\text{CN})_6$ was successfully synthesized by a simple and cost effective route. Advantages of this method are that no inert atmosphere and no high temperature are required during synthesis [45-48]. Secondly, the material is non-toxic [35], and shows good cyclic ability, when used in rechargeable lithium-ion battery as cathode material. Low capacity fading upon cycling is observed at low drain discharge condition. Finally, it can be used as liquid cathode [37], in aqueous lithium ion battery, since it is soluble in water.

COMPETING INTEREST

Authors have declared that no competing interests exist.

REFERENCES

1. Sadoway DR, Mayes AM. Portable Power: Advanced Rechargeable Lithium Batteries. MRS Bull. 2002;27:590-596.
2. Miao C, Bai P, Jiang Q, Sun S, Wang X. A novel synthesis and Characterization of LiFePO_4 and LiFePO_4/C as a cathode material for lithium-ion battery. *J. Power Sources*. 2014;246:232-238.
3. Patil A, Patil V, Shin DW, Choi J-W, Paik D-S, Yoon S-J. Issue and challenges facing rechargeable thin film lithium batteries. Mater. Res. Bull. 2008;43:1913-1942.
4. Fergus JW. Recent developments in cathode materials for lithium ion batteries. *J. Power Sources*. 2010;195:939-954.
5. Liu C, Nan J, Zuo X, Xiao X, Shu D. Synthesis and Electrochemical Characteristics of an Orthorhombic LiMnO_2 Cathode Material Modified With Poly(Vinyl-Pyrrolidone) for Lithium Ion Batteries. *Int. J. Electrochem. Sci*. 2012;77:7152-7164.

6. Ammundsen B, Desilvestro J, Groutso T, Hassell D, Metson JB, Regan E, Steiner R, Pickering PJ. Formation and Structural Properties of Layered LiMnO_2 Cathode Materials. *J. Electrochem. Soc.* 2000;147:4078-4082.
7. Vitins G, West K. Lithium Intercalation into Layered LiMnO_2 . *J. Electrochem. Soc.* 1997;144:2587-2592.
8. Kim DK, Muralidharan P, Lee HW, Ruffo R, Yang Y, Chan CK, Hailin P, Huggins RA, Cui Y. Spinel LiMn_2O_4 Nanorods as Lithium Ion Battery Cathodes. *Nano Lett.* 2008;8:3948–3952.
9. Zhao X, Reddy MV, Liu H, Ramakrishna S, Subba Rao GV, Chowdari BVR. Nano LiMn_2O_4 with spherical morphology synthesized by a molten salt method as cathodes for lithium ion batteries. *RSC Adv.* 2012;2:7462-7469.
10. Lee S, Cho Y, Song HK, Lee KT, Cho J. Carbon-Coated Single-Crystal LiMn_2O_4 Nanoparticle Clusters as Cathode Material for High-Energy and High-Power Lithium-Ion Batteries. *Angew. Chem.* 2012;51:8748–8752.
11. Chen Z, Du B, Xu M, Zhu H, Li L, Wang W. Polyacene coated carbon/ LiFePO_4 cathode for Li ion batteries: Understanding the stabilized double coating structure and enhanced lithium ion diffusion kinetics. *Electrochim. Acta.* 2013;109:262-268.
12. Wu G, Zhou Y, Shao Z. Carbon nanotube and graphene nanosheet co-modified LiFePO_4 nanoplate composite cathode material by a facile polyol process. *Appl. Surf. Sci.* 2013;283:999-1005.
13. Yang X, Xu Y, Zhang H, Huang Y, Jiang Q, Zhao C. Enhanced high rate and low-temperature performances of mesoporous LiFePO_4 /Ketjen Black nanocomposite cathode material. *Electrochim. Acta.* 2013;114:259-264.
14. Chen T-K, Qi X, Chen C-Y, Chang C-C, Chang W-C. Maleic-anhydride-grafted ketjen black as the alternative carbon additive for LiFePO_4 cathode. *Electrochim. Acta.* 2013;107:503-508.
15. Maccario M, Croguennec L, Cras F, Delmas C. Electrochemical performances in temperature for a C-containing LiFePO_4 composite synthesized at high temperature. *J. Power Sources.* 2008;183:411-417.
16. Murugan AV, Muraliganth T, Manthiram A. Rapid microwave-solvothermal synthesis of phospho-olivine nanorods and their coating with a mixed conducting polymer for lithium ion batteries. *Electrochem. Commun.* 2008;10:903-906.
17. Mandal B, Basumallick I, Ghosh S. One pot synthesis of Zr^{4+} doped carbon coated LiFePO_4 cathode material for rechargeable Li-ion battery. *British J. Appl. Sci. Tech.* 2014;4(10):1509-1519.
18. Wang GX, Bewlay S, Needham SA, Liu HK, Liu RS, Drozd VA, Lee JF, Chen JM. Synthesis and Characterization of LiFePO_4 and $\text{Li}_{0.99}\text{Ti}_{0.01}\text{Fe}_{0.99}\text{PO}_4$ Cathode Materials. *J. Electrochem. Soc.* 2006;153:A25-A31.
19. Chung SY, Chiang YM. Microscale Measurements of the Electrical Conductivity of Doped LiFePO_4 . *Electrochem. Solid-St. Lett.* 2003;6:A278-A281.
20. Jayaprakash N, Kalaiselvi N, Periasamy P. Synthesis and Characterization of $\text{LiMXFe}_{1-x}\text{PO}_4$ (M = Cu, Sn; X = 0.02) Cathodes - A study on the Effect of Cation Substitution in LiFePO_4 Material. *Int. J. Electrochem. Sci.* 2008;3:476-488.
21. Roberts MR, Spong AD, Vitins G, Owen JR. High Throughput Screening of the Effect of Carbon Coating in LiFePO_4 Electrodes. *J. Electrochem. Soc.* 2007;154:A921-A928.
22. Kuwahara A, Suzuki S, Miyayama M. Hydrothermal synthesis of LiFePO_4 with small particle size and its electrochemical properties. *J. Electroceram.* 2010;24:69-75.
23. Kanamura K, Koizumi S, Dokko K. Hydrothermal synthesis of LiFePO_4 as a cathode material for lithium batteries. *J. Mater. Sci.* 2008;43 2138–2142.
24. Lee J, Teja AS. Synthesis of LiFePO_4 micro and nanoparticles in supercritical water. *Mater. Lett.* 2006;60:2105–2109.
25. Kim DH, Kim J. Synthesis of LiFePO_4 nanoparticles and their electrochemical properties. *J. Phys. Chem. Solids.* 2007;68:734–737.
26. Qin X, Wang X, Xiang H, Xie J, Li J, Zhou Y. Mechanism for Hydrothermal Synthesis of LiFePO_4 Platelets as Cathode Material for Lithium-Ion Batteries. *J. Phys. Chem. C.* 2010;114:16806–16812.
27. Xu Z, Xu L, Lai Q, Ji X. A PEG assisted sol–gel synthesis of LiFePO_4 as cathodic material for lithium ion cells. *Mater. Res. Bull.* 2007;42:883–891.
28. Yang J, Xu JJ. Synthesis and Characterization of Carbon-Coated Lithium Transition Metal Phosphates LiMPO_4 (M=Fe, Mn, Co, Ni) Prepared via a Nonaqueous Sol-Gel Route. *J. Electrochem. Soc.* 2006;153:A716-A723.

29. Lee SB, Cho SH, Cho SJ, Park GJ, Park SH, Lee YS. Synthesis of LiFePO_4 material with improved cycling performance under harsh conditions. *Electrochem. Commun.* 2008;10:1219–1221.
30. Lin Y, Pan H, Gao M, Miao H, Li S, Wang Y. Synthesis and characterization of LiFePO_4/C prepared via sol-gel method. *Surf. Rev. Let.* 2008;15:133–138.
31. Jugovic D, Mitric M, Cvjetanin N, Janear B, Mentus S, Uskokovic D. Synthesis and characterization of LiFePO_4/C composite obtained by sonochemical method. *Solid St. Ionics.* 2008;179:415–419.
32. Yang H, Wu XL, Cao MH, GuoYG. Solvothermal Synthesis of LiFePO_4 Hierarchically Dumbbell-Like Microstructures by Nanoplate Self-Assembly and Their Application as a Cathode Material in Lithium-Ion Batteries. *J. Phys. Chem. C.* 2009;113:3345–3351.
33. Recham N, Dupont L, Courty M, Djellab K, Larcher D, Armand M, Tarascon JM. Ionothermal Synthesis of Tailor-Made LiFePO_4 Powders for Li-Ion Battery Applications. *Chem. Mater.* 2009;21:1096–1107.
34. Beninati S, Damen L, Mastragostino M. MW-assisted synthesis of LiFePO_4 for high power applications. *J. Power Sources.* 2008;180:875–879.
35. Qian J, Zhou M, Cao Y, Ai X, Yang H. Nanosized $\text{Na}_4\text{Fe}(\text{CN})_6/\text{C}$ Composite as a Low-Cost and High-Rate Cathode Material for Sodium-Ion Batteries. *Adv. Energy Mater.* 2012;2:410–414.
36. [Wikipedia], http://en.wikipedia.org/wiki/Potassium_ferrocyanide.
37. Wang X, Hou Y, Zhu Y, Wu Y, Holze R. An Aqueous Rechargeable Lithium Battery Using Coated Li Metal as Anode. *Sci. Rep.* 2013;3:1401, doi: 10.1038/srep01401, 1-5.
38. [Wikipedia], <http://en.wikipedia.org/wiki/KCFO4>.
39. Harish S, Joseph J, Phani KLN. Interaction between gold (III) chloride and potassium hexacyanoferrate (II/III)—Does it lead to gold analogue of Prussian blue? *Electrochim. Acta.* 2011;56:5717–5721.
40. Chakrabarty MH, Roberts EPL. Analysis of Mixtures of Ferrocyanide and Ferricyanide using UV-Visible Spectroscopy for Characterisation of a Novel Redox Flow Battery. *J. Chem. Soc. Pak.* 2008;30(6):817–823.
41. Hussain S, Betsch K, LaCroix C. Available: <http://ed.augie.edu/~calacroi/irramanlab.html>.
42. Klyuev YA. Vibrational Spectra of crystalline potassium ferri- and ferrocyanide. *J. Appl. Spectrosc.* 1965; 3:30–34.
43. Idemura S, Suzuki E, Ono Y. Electronic state of iron complexes in the interlayer of hydrotalcite-like materials. *Clays Clay Miner.* 1989; 37:553–557.
44. Balmaseda J, Reguera E, Fernandez J, Gordillo A, Yee-Madeira H. Behavior of Prussian blue-based materials in presence of ammonia. *J. Phys. Chem. Solid.* 2003;64:685–693.
45. Nakamura T, Miwa Y, Tabuchi M, Yamada Y. Structural and Surface Modifications of LiFePO_4 Olivine Particles and Their Electrochemical Properties. *J. Electrochem. Soc.* 2006;153(6):A1108–A1114.
46. Lim S, Yoon CS, Cho J. Synthesis of Nanowire and Hollow LiFePO_4 Cathodes for High-Performance Lithium Batteries. *Chem. Mater.* 2008;20:4560–4564.
47. Bilecka I, Hintennach A, Djerdj I, Novak P, Niederberger M. Efficient microwave-assisted synthesis of LiFePO_4 mesocrystals with high cycling stability. *J. Mater. Chem.* 2009;19:5125–5128.
48. Dominko R, Bele M, Goupil JM, Gaberscek M, Hanzel D, Arcon I, Jamnik J. Wired Porous Cathode Materials: A Novel Concept for Synthesis of LiFePO_4 . *Chem. Mater.* 2007;19:2960–2969.